DFT Description of the Electronic Structure and Spectromagnetic Properties of Strongly Correlated Electronic Systems: Ni^{II}, Cu^{II} and Zn^{II} *o*-Dioxolene Complexes

Alessandro Bencini,* Chiara Carbonera,* and Federico Totti*[a]

Abstract: The spectroscopic and magnetic properties of dioxolene complexes of zinc, copper and nickel were studied by DFT calculations on model complexes of formulas $[(NH_3)_4M^{II}(SQ)]^+$ (M = Zn, Ni; SQ = semiquinonato) and $[(NH_3)_2Cu^{II}(SQ)]^+$. Standard approaches such as time-dependent DFT (TDDFT), the Slater transition state (STS), and broken symmetry (BS) were found to be unable to completely account for the physical properties of the systems, and complete active space-configuration interaction (CAS-CI) calculations based on the Kohn–Sham (KS) orbitals was applied. The CAS-CI energies, properly corrected with multireference perturbation theory (MR-PT), were found to be in good agreement with experimental data. We present here a calculation protocol that has a low CPU cost/accuracy ratio and seems to be very promising for interpreting the properties of strongly correlated electronic systems in complexes of real chemical size.

Keywords: ab initio calculations · charge transfer · density functional calculations · magnetic properties · semiquinone complexes

Introduction

Density functional theory (DFT) has been widely used in the last few years to calculate structural and spectromagnetic properties of a large range of substances, from isolated molecules to extended solids.[1] The success of DFT lies in its ability to handle systems that reach real chemical complexity with a low CPU cost/accuracy ratio. The use of the generalized gradient approximation (GGA)[2] and the adiabatic connection formula (ACF)[3] significantly improved the quality of the results and led to better agreement with experiment. Much attention was devoted to the study of magnetic interactions in molecular magnets, a field in which an accurate treatment of the electron correlation is required and where modelling of the external ligands can produce incorrect absolute values of the exchange coupling constants.[4] Among the paramagnetic systems synthesized so far and studied as building blocks for molecular magnetic materials,[5,6] complexes of polyoxolene radical ligands and transition metal ions occupy a special place, since they show rich chemistry associated with their redox properties together with magnetic activity.[7] The *o*-dioxolene ligands in particular can exist in the three redox forms quinone (Q), semiquinonato anion (SQ^-) and catecholato dianion (CAT^{2-}), and their complexes with Mn and Co can exhibit different ground states depending on environmental conditions such as pressure and temperature. This phenomenon, which resembles the well-known spin equilibrium observed in a number of transition metal complexes, is generically called valence tautomerism.[8] In a localized description of the chemical bond, the variation of the ground state in these complexes can be seen as an interconversion between two localized electronic structures that can be described, for example, as $[M^{II}(SQ)]^+$ and $[M^{III}(CAT)]^+$. Studying the electronic structure of these systems is therefore rather complex. Indeed, in addition to the formal assignment of the oxidation states, the equilibrium between high- and low-spin forms of the metal ions and the exchange interactions between the unpaired electron on SQ^- and those on the metal ions must be correctly described. It is therefore not surprising that these systems show unusual physical and chemical properties. It was shown experimentally that the formal oxidation states of the complexes can be reasonably established by examining the C–O and C–C bond lengths of the *o*-dioxolene ligands, which are strongly dependent on the formal charge of the ligands.[8,9] Typical values are $d_{CO} = 1.35$ Å and $d_{CC} = 1.39$–1.40 Å for CAT^{2-} species, $d_{CO} = 1.29$–1.30 Å and $d_{CC} = 1.44$ Å for SQ^- species, and $d_{CO} = 1.23$ Å and $d_{CC} = 1.49$–1.50 Å for Q species. Assignment of the formal oxidation states by using the above empirical rules greatly helps in understanding the overall properties of these substances, but a more exact approach is required to achieve a quantitative description of their chemical and physical properties, and to predict new physical and chemical behaviours.

[a] Prof. A. Bencini, Dr. C. Carbonera, Dr. F. Totti
Dipartimento di Chimica, via della Lastruccia 3
Università di Firenze, Sesto Fiorentino (FI) (Italy)
Fax: (+39)055 4573372
E-mail: alessandro.bencini@unifi.it

DOI: 10.1002/chem.200305420

Density functional theory[10] has been recently applied with some success to calculate several aspects of the chemistry and physics of metal *o*-dioxolene complexes, and particularly the reproduction of the magnetic properties of a number of systems showed that the method is appropriate to describe the ground and the next excited state of these systems.[11] However, a deeper characterization of their properties requires knowledge of the energies and geometries of higher excited states. A DFT description of the excited states of $[Co^{II}(SQ)_2(phen)]$, particularly those responsible for valence tautomerism, has been published,[11a] and more recently we applied DFT to describe the electronic structure of simpler Co^{II} semiquinonato complex.[12] Although some important information has been obtained on these systems, some discrepancy with experimental data was found, and a deeper investigation is needed. The main drawback of DFT in describing the electronic states of metal semiquinonato complexes is due to the single-determinant (SD) picture, which can be inadequate for nearly degenerate electronic states. The electronic structure of these systems is indeed characterized by a manifold of low-energy electronic states, which can be thermally populated and, in an approach by wavefunction theory, should be described by multireference (MR) wavefunctions such as those obtained by complete-active-space (CAS) configuration interaction (CI) self-consistent field (SCF) calculations. LaBute et al.[13] recently corrected the results of DFT calculations on cobalt valence tautomers using a variational configuration interaction approach based on a model Hamiltonian. General approaches to combine multideterminant wavefunctions with DFT are currently under development,[14] and recently PBour[15] corrected the Kohn–Sham (KS) wavefunctions with CI and thus obtained a significant improvement over the HF results in a number of systems. Although the direct correction of KS wavefunctions with CI can lead to some overestimation of the electron correlation, the procedure can be applied in a straightforward way with available computer code, and the results obtained by Bour prompted us to investigate the application of this procedure to metal–semiquinonato systems.

Here we apply the MR-CI/KS formalism to calculate the electronic structure, magnetic properties and electronic spectra of a series of M^{II} *o*-dioxolene model complexes of formulas $[(NH_3)_4M^{II}(SQ)]^+$ (M = Zn, Ni; SQ = semiquinonato) and $[(NH_3)_2Cu^{II}(SQ)]^+$. Ammonia molecules were used to mimic the effect of the more complex nitrogen ligands (usually CTH = *dl*-5,7,7,12,14,14-hexamethyl-1,4,8,11-tetraazacyclotetradecane), which are present in the real compounds. The complexes studied here are not expected to undergo valence tautomerism, since the excited M^{III}–catecholato forms should lie at energies higher than the thermal quantum at room temperature because of their redox potentials. However, complexes of formulas $[(CTH)M^{II}(SQ)]^+$ have been widely characterized[7,11f,16] by magnetic and spectroscopic techniques, as well as by X-ray diffraction, and offer numerous experimental data that can be used to test the MR-CI/KS approach. These systems therefore seem well suited as tests for calculations aimed at establishing a general procedure to be applied to systems of chemical dimensions. In the following, we compare MR-CI/KS with other standard DFT procedures to calculate the magnetic properties and electronic spectra of the model complexes $[(NH_3)_4M^{II}(SQ)]^+$ and $[(NH_3)_2Cu^{II}(SQ)]^+$ and test the accuracy of the methods on the available experimental data for the real parent complexes.

Methods of Calculation

DFT calculations were performed with Slater-type orbitals (STO) using the Amsterdam Density Functional program package (ADF2002),[17] and with Gaussian-type orbitals (GTO) using the General Atomic and Molecular Electronic Structure System (GAMESS)[18] and the NWChem[19] program packages on the model complexes of formulas $[(NH_3)_4M(SQ)]^+$ (M = Zn, Ni) and $[(NH_3)_2Cu(SQ)]^+$ shown in Figure 1. C_{2v} symmetry was assigned to all the complexes. STOs were used in the form of double-ζ orbitals for the core electrons, and triple-ζ orbitals for the valence electrons plus one polarization function for all the metals; double-ζ orbitals plus one polarization function were applied to all the other atoms, except hydrogen atoms, for which no polarization was added. Coefficients and exponents of the basis functions were taken from the standard database of ADF2002. Metal electrons up to the 2p shell were kept frozen. For all the other non-hydrogen atoms the 1s shell electrons were frozen. GTO calculations were performed with the all-electron basis sets developed by Ahlrichs et al.[20] as obtained from the Extensible Computational Chemistry Environment Basis Set Database.[21] Triple-ζ functions were used for the metal atoms and double-ζ functions were applied to all the other atoms.

Geometry optimizations: The geometries of the model complexes were optimized with ADF by using the Vosko–Wilks–Nusair formula (version V)[22] for the local density approximation (LDA) part of the exchange-correlation functional and the nonlocal (GGA) corrections of Becke[23] and Perdew[24] to the exchange and correlation part of the functional, respectively. This functional is indicated by the abbreviation BP below. The Broyden–Fletcher–Goldfarb–Shanno (BFGS) Hessian update was used throughout, and default criteria of convergence on energy, displacements and gradients were applied. Optimizations were always performed on the highest spin state of each system, since it can be meaningfully described by a single Slater determinant. Dihedral angles between the hydrogen atoms of the NH_3 ligands were fixed to impose a local C_3 axis around the M–N bond.

Magnetic properties: The exchange coupling constant J between the metal ion and the semiquinonato radical was calculated by using the broken symmetry formalism (BS), as described at length in the literature.[25] In this approach J is obtained from two independent SCF calculations: the first on the highest spin state of the system (the ferromagnetic state, F), and the second on the antiferromagnetic state (AF), in which the metal ion is in its internal highest spin state with α electrons, and the electron on the SQ^- radical has spin β. The exchange coupling constant of the spin Hamiltonian[26] $H = J\boldsymbol{S}_M \cdot \boldsymbol{S}_{SQ}$ can be calculated from the energies of these two single determinants, E(F) and E(AF) according to Equation (1), where S_M is the total spin on the metal centre and $S_{SQ} = 1/2$.

$$J = \frac{E(\mathrm{F}) - E(\mathrm{AF})}{2 S_M S_{SQ}} \qquad (1)$$

This equation results from the projection of the AF state, which is not an eigenfunction of $\boldsymbol{S}^2$, onto the pure spin state corresponding to the antiferromagnetic alignment of the magnetic electrons. The use of Equation (1) most often leads to an overestimation of the calculated J value with respect to the experimental values, and sometimes the AF (or BS) state was instead considered as a pure spin state.[27] For two $S = 1/2$ spins, this approach means that the factor of 2 in the denominator is omitted. Both approaches are considered in this paper.

Modelling the external CTH ligand with NH_3, although justified, since in both cases the bonding atoms are tertiary nitrogen atoms, and already

practiced in the literature,[11d,28] can alter the absolute value of the calculated J and prevents their quantitative agreement with the experimental data.[29] Furthermore, small deviations of bond lengths and angles from the real values can affect the actual value of J, and the agreement with the experimental data presented in this paper can therefore be considered good when the sign and the order of magnitude of J is reproduced.

Other excited states: Energies of excited states were calculated in more general ways by using DFT based methods and MR-CI/KS calculations.

The Slater transition state[30] (STS) procedure was applied to calculate the energy of excited states having the same spin multiplicity as the ground state that originate from one-electron excitations from the ground-state single Slater determinant. All these calculations were performed with ADF.

The reference configurations of the MR-CI/KS approach were chosen within a complete active space (CAS), and we also refer to these calculations as CAS-CI calculations. The states obtained from the CAS-CI were the zeroth-order states of a second-order perturbation approach. MR-CI/KS calculations[31] were performed with GAMESS using as reference space the KS orbitals obtained from DFT/restricted open shell (DFT/RO) calculations with the B3LYP hybrid functional,[32] as described in more detail below. The results of the CAS-CI calculations were corrected for dynamic correlation effects by using the multireference second-order perturbation theory[33] (MR-PT), as implemented in GAMESS, with the multireference quasidegenerate perturbation theory approach[34] (MC-QDPT) applied to a single zeroth order state at the time. Intruder states were eliminated by using an energy denominator shift[35] in the perturbation expression of $\delta = 0.0011$ a.u. for all the states.

Time-dependent DFT[36] (TDDFT) in the Tamm–Dancoff approximation,[37] as implemented in NWChem, was also applied. Oscillator strengths of the allowed transitions were calculated from CAS-CI and TDDFT calculations.

UV/Vis spectra were calculated using the results of MR-PT calculations by broadening each absorption transition at ω_0 with a Gaussian function according to Equation (2), where f_{ω_0} is the oscillator strength, and w_{ω_0} the bandwidth.

$$g(\omega) = \frac{f_{\omega_0}}{w_{\omega_0}}\sqrt{\frac{2}{\pi}}e^{-2(\omega-\omega_0)^2/w^2_{\omega_0}} \quad (2)$$

The bandwidths were arbitrarily chosen to mimic the features of the experimental spectra.

Details of the calculations: All calculations were performed on an eight-node AMD Athlon 2000 double-processor cluster. The most expensive calculations (MR-PT) were performed on four processors using 320 MB RAM on each node with 60 min (average) total CPU time.

Results and Discussion

The geometries of the model complexes $[(NH_3)_4M^{II}(SQ)]^+$ (M = Zn, Ni) and $[(NH_3)_2Cu^{II}(SQ)]^+$ calculated with ADF/BP are shown in Figure 1, together with relevant geometrical parameters. The calculations were performed on the highest spin state of each molecule, namely, $S = 1/2$ for $[(NH_3)_4Zn(SQ)]^+$, $S = 1$ for $[(NH_3)_2Cu(SQ)]^+$ and $S = 3/2$ for $[(NH_3)_4Ni(SQ)]^+$. These spin states were found to be the ground spin states of each system, in agreement with the observed magnetic properties of the analogous real complexes. The C–O and C–C bond lengths are close to those experimentally observed for semiquinonato species and allow the assignment of a 2+ formal charge to the metal centres. The bond lengths around the metal atoms compare favourably with those reported in the literature,[7,38] except for the Ni–O bonds, which are somewhat shorter than the experimental values (2.06–2.08 Å).[11f] The charge and spin densities calculated by Mulliken population analysis are reported in Table 1. The spin densities are quite well localized onto the $[M(NH_3)_n]$ and SQ fragments: 0.17 and 0.30 electrons are transferred from the metal to the semiquinonato ligand in the Ni and Cu complexes, respectively. These findings suggest that the usual spin Hamiltonian approach, which is based on a localized picture of the spin of the unpaired electrons, can be a valid tool for rationalizing the magnetic properties in these systems.

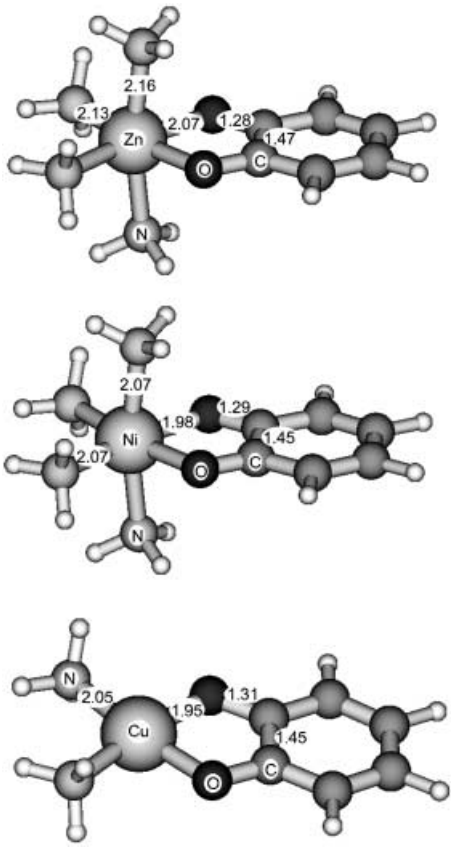

Figure 1. Optimized structures of model complexes $[(NH_3)_4M(SQ)]^+$ (M = Zn, Ni; SQ = semiquinonato) and $[(NH_3)_2Cu(SQ)]^+$. The relevant geometrical parameters are shown.

Table 1. Charges and spin densities calculated[a] for $[(NH_3)_4Zn(SQ)]^+$, $[(NH_3)_4Ni(SQ)]^+$ and $[(NH_3)_2Cu(SQ)]^+$.

Atoms	Charge	Spin density
Zn	0.66	−0.01
$(NH_3)_4$	0.89	0.02
SQ	−0.55	0.99
Ni	0.58	1.47
$(NH_3)_4$	0.92	0.37
SQ	−0.50	1.17
Cu	0.84	0.52
$(NH_3)_2$	0.48	0.18
SQ	−0.32	1.30

[a] Results of ADF/BP calculations. Atomic contribution were added to form the relevant fragments.

The compositions of the SOMOs and of two of the lower unoccupied orbitals for the three complexes are shown in Figure 2 as isosurface plots of the relevant wavefunctions with $\psi = \pm 0.05$ a.u. An MO localized on the ammonia molecules was found to be the LUMO in all complexes and is

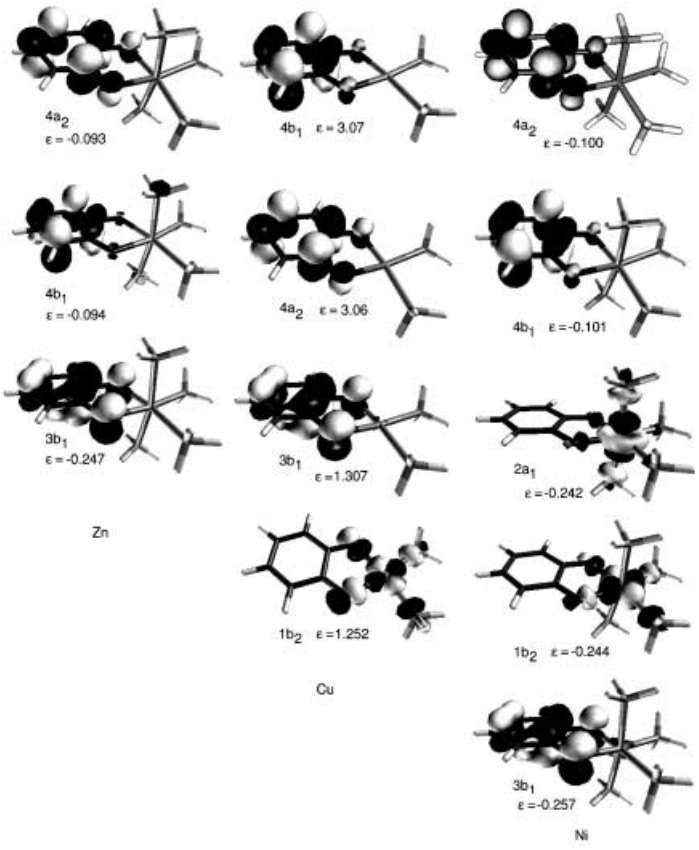

Figure 2. Isosurface plots ($\psi = \pm 0.05$ a.u.) of the SOMOs and of two of the unoccupied orbitals ($4b_1$ and $4a_2$) for $[(NH_3)_4M(SQ)]^+$ (M = Zn, Ni) and $[(NH_3)_2Cu(SQ)]^+$.

not shown. The $4b_1$ and $4a_2$ orbitals shown in Figure 2 are therefore the LUMO + 1 and LUMO + 2 orbitals.

For the zinc(II) complex, the orbitals shown in Figure 2 closely resemble those calculated in the HOMO-LUMO region for the SQ^- radical anion by DFT calculations on the free radical using the same atomic coordinates as found in $[(NH_3)_4Zn(SQ)]^+$. The electronic structure of the semiquinonato radical anion has already been studied in some detail[39] and will not be described here. The 3d orbitals in the zinc(II) complex lie quite low in energy and are doubly occupied. It is evident that charge transfer from the metal to the HOMO $3b_1$ orbital, which can be described as Zn^{III}–CAT states, are expected to be high in energy.

The contribution of the 3d orbitals to the magnetic and redox properties of the complexes becomes more important in the copper(II) and nickel(II) complexes, for which the $1b_2$ and $2a_2$ orbitals, mainly centred on the metal ion, enter the SOMO region, as shown in Figure 2. In the copper(II) complex the magnetic orbitals are $1b_2$ and $3b_1$. Charge-transfer states originating from electron transfer between these two orbitals are expected to be the low-lying Cu^{III}–CAT ($1b_2^0\ 3b_1^2$) and Cu^{I}–Q ($1b_2^2\ 3b_1^0$) configurations, while the singlet ($^1A_2$) and triplet ($^3A_2$) states, arising from the ground ($1b_2^1\ 3b_1^1$) configuration, give rise to the magnetic properties of the complex. A more complicated magnetic and redox behaviour is expected for the nickel(II) complex. From the ground ($3b_1^1\ 1b_2^1\ 2a_1^1$) configuration one quartet ($^4A_2$) and two doublet ($^2A_2$) states arise, which are responsible for the magnetic properties. Charge-transfer between the ground configuration give rise to Ni^{III}–Cat [$^2B_2 \in (3b_1^0\ 1b_2^1\ 2a_1^2)$] and [$^2A_1 \in (3b_1^0\ 1b_2^2\ 2a_1^1)$], and Ni^{I}–Q [$^2B_2 \in (3b_1^2\ 1b_2^1\ 2a_1^0)$ and $^2A_1 \in (3b_1^2\ 1b_2^0\ 2a_1^1)$] states. Other configurations arising from excitations from lower lying states are also possible, and it is evident that, since many states have the same spin and space symmetry, only methods allowing for static electron correlation effects, that is, for multideterminant states, can be appropriate for describing the electronic structure of the nickel(II) complex.

Multiplet structure of $[(NH_3)_4Zn^{II}(SQ)]^+$ and SQ^-: To apply MR methods, an appropriate interaction space (complete active space) must be chosen. A minimum active space would be that formed by the 3d metal orbitals and the $3b_1$ orbital of the semiquinonato anion, as already chosen by La Bute et al.[13] in a different context. However, this active space cannot account for the UV spectrum of the zinc(II) complex, for example, whose interpretation requires at least that all low-lying states of SQ^- lie in the active space, according to the assignment by Dei et al.[40] In order to have a "spectroscopic" active space we added to the minimum active space the highest energy KS MOs of SQ^- to yield a 13-orbital active space. The orbitals forming this complete active space (CAS) used for the CAS-CI/KS calculations on $[(NH_3)_4Zn(SQ)]^+$ are shown in Figure 3 as an isosurface plot with $\psi = \pm 0.05$ a.u. together with their symmetry labels and numbering. In the calculations on the other metal complexes we used the same numbering of the energy levels in order to quickly compare transitions arising from homologous orbitals between different metal complexes. The CAS include two σ-like ($1b_2$, $2a_1$) and three π-like ($1a_1$, $1b_1$, $1a_2$) 3d metal orbitals; all the π-type MOs of the semiquinonato ligand with relevant contributions from the oxygen atoms at higher energies ($2a_2$, $2b_1$, $3a_2$, $3b_1$); the two low-lying empty orbitals of SQ^- ($4b_1$, $4a_2$); and the two highest occupied σ-type orbitals of SQ^- ($2b_2$, $3a_1$) that have the appropriate symmetry to interact with $3d_\sigma$ atomic orbitals.

We tested the quality of the active space by calculating the electronic excitations in the zinc(II) complex and in the free semiquinonato ligand. The results of the calculations are reported in Tables 2 and 3. In Figure 4 the calculated spectra are compared with the UV/Vis electronic spectrum[40] of [Zn(*SS*-CTH)(DTBSQ)]PF_6 (*SS*-CTH = (*S*,*S*)-5,5,7,12,12,14-hexamethyl-1,4,8,11-tetraazacyclotetradecane; DTBSQ = anion of 3,5-di-*tert*-butylbenzo-*o*-semiquinone). The spectra were obtained by plotting the transition energies obtained by MR-PT calculations with oscillator strengths calculated on the CAS-CI zeroth order states according to the procedure described in the Methods of Calculation. The reference space for the calculations on the zinc

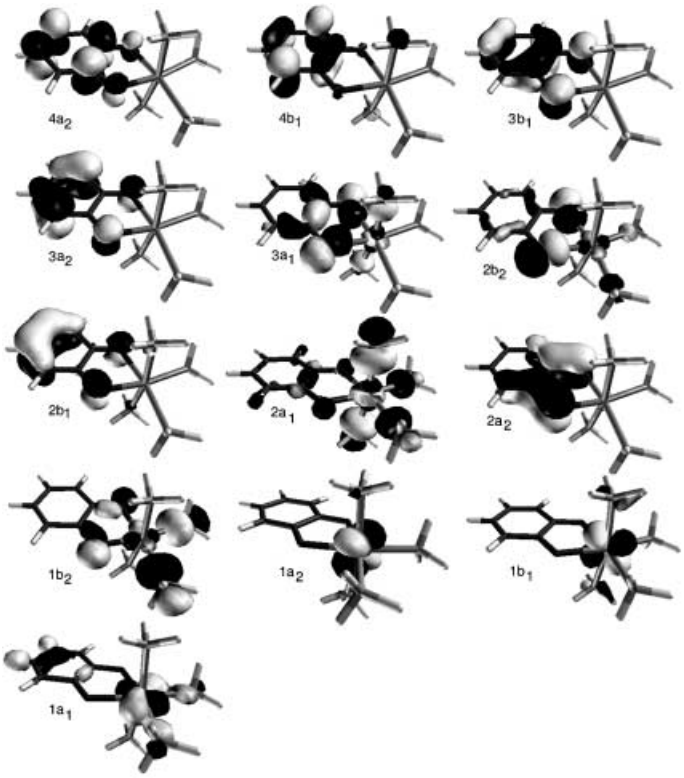

Figure 3. CAS used for MR-CI/KS calculations on $[(NH_3)_4Zn(SQ)]^+$. Isosurface plot of the relevant wavefunctions with $\psi = \pm 0.05$ a.u. The same symmetry labels and numbering scheme was used in the CAS-CI calculations on all the other model systems.

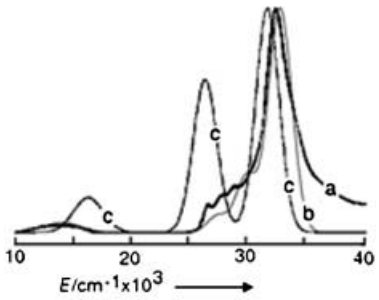

Figure 4. a) UV/Vis electronic spectrum of [Zn(*SS*-CTH)(DTBSQ)]PF_6 (*SS*-CTH = (*S*,*S*)-5,5,7,12,12,14-hexamethyl-1,4,8,11-tetraazacyclotetradecane; DTBSQ = anion of 3,5-di-*tert*-butylbenzo-*o*-sequinone). b) Spectrum of $[(NH_3)_4Zn(SQ)]^+$ calculated with MR-PT/KS. c) Spectrum of the SQ^- radical anion calculated with MR-PT/KS.

Table 2. Calculated electronic transitions [cm^{-1}] for $[Zn(NH_3)_4(SQ)]^+$.

Transition	CAS[a]	MR-PT	Transition[b]
$^2B_1 \rightarrow {}^2A_2$	18330 (2.8)	14061	$3a_2 \rightarrow 3b_1$
$^2A_1$	26731 (0.0)	15746	$3a_1 \rightarrow 3b_1$
$^2B_2$	32988	16966	$2b_2 \rightarrow 3b_1$
$^2B_1$	37700 (2.6)	27345	$2b_1 \rightarrow 3b_1$[c]
$^2A_2$	41843 (8.6)	29812	$3b_1 \rightarrow 4a_2$
$^2A_2$	49934 (22.7)	32366	$2a_2 \rightarrow 3b_1$
$^2B_1$	**46647 (15.3)**	**33208**	**$3b_1 \rightarrow 4b_1$**[c]
$^2B_2$	63042	42624	$3a_1 \rightarrow 4a_2$
$^2A_1$	68067 (0.4)	45970	$3a_2 \rightarrow 4a_2$
$^2B_1$	69564 (8.9)	45977	$1b_2 \rightarrow 3a_2$
$^2A_1$	70030 (0.0)	47093	$2b_2 \rightarrow 4a_2$
$^2A_2$	65150 (7.5)	47101	$3a_2 \rightarrow 4b_1$
$^2B_2$	72115	52137	$2b_2 \rightarrow 4b_1$

[a] Transition energies from configuration interaction on the CAS(13/21) reference space. Transitions $2B_1 \rightarrow 2B_2$ are symmetry forbidden. Oscillator strength (length form [a.u. × 100]) in parentheses. [b] Main one-electron excitation from the reference state. [c] The $^2B_1$ states from the SOMO–LUMO ($3b_1 \rightarrow 4b_1$) and ($2b_1 \rightarrow 3b_1$) transitions are strongly admixed by configuration interaction. The calculated coefficients in the CI expansions are: $0.74(2b_1 \rightarrow 3b_1) + 0.52(3b_1 \rightarrow 4b_1)$ and $0.44(2b_1 \rightarrow 3b_1) - 0.72(3b_1 \rightarrow 4b_1)$ for the transitions at 27345 and 33208 cm^{-1}, respectively. SOMO–LUMO transition is in boldface.

complex contains 21 active electrons, CAS(13/21), and that for the SQ^- radical is CAS(8/11). Electronic transitions to B_2-symmetry states are forbidden in C_{2v}, but can appear as extra bands in the experimental spectra due to the lower symmetry of the complexes. The intensities of these transitions, as well as those of the transitions to A_1 states, which were calculated with zero oscillator strengths, are expected to be low, and these transitions should appear as shoulders on the main absorptions. The overall agreement between the calculated spectrum for the zinc complex and the experimental one is apparent.

For comparison, we also calculated the transition energies of the SQ^- ligand with other theoretical methods (Table 3). The first correction to the energies of the CAS-CI states was obtained by allowing configuration interaction with all 48 virtual orbitals (FOCI calculations). We thus introduce into our states all the dynamical correlation effects coming from the virtual orbitals. Two DFT approaches, namely, STS and TDDFT, were also applied. Dy-

Table 3. Comparison between calculated electronic transitions [cm^{-1}] for SQ^- with different theoretical methods.

Transition	CAS[a]	FOCI[b]	MR-PT	Transition[c]	STS	TDDFT[d]
$^2B_1 \rightarrow {}^2A_1$	16906 (0.0)	15105 (0.0)	9886			
$3a_1 \rightarrow 3b_1$	9810	11516 (0.0)				
$^2B_2$	21159	18597	12612	$2b_2 \rightarrow 3b_1$	13726	15370
$^2A_2$	19873(4.2)	18971(3.4)	16290	$3a_2 \rightarrow 3b_1$	15536	20765 (2.6)
$^2B_1$	**32433 (3.6)**	**30833 (3.5)**	**25982**	**$3b_1 \rightarrow 4b_1$**	**27870**	**32318 (2.6)**
$^2A_2$	35111(11.8)	32252(8.6)	26420	$3b_1 \rightarrow 4a_2$	29142	34335 (4.3)
$^2B_1$	46939 (13.3)	42685 (8.3)	31650	$2b_1 \rightarrow 3b_1$	34068	40001 (6.2)
$^2A_2$	43732 (13.3)	39987 (9.1)	31626	$2a_2 \rightarrow 3b_1$	33109	40667 (18)
$^2A_1$	47350 (0.1)	44174 (0.0)	33273	$3a_1 \rightarrow 4b_1$	36042	37396 (0.0)
$^2B_2$	48500	44962	34981	$3a_1 \rightarrow 4a_2$	37409	39377
$^2B_2$	50383	46903	35033	$2b_2 \rightarrow 4b_1$	40881	42472
$^2A_1$	52295 (0.1)	48281 (0.0)	36639	$2b_2 \rightarrow 4a_2$	41785	45331 (0.0)

[a] Transition energies from configuration interaction on the CAS(8/11) reference space. Transitions $2B_1 \rightarrow 2B_2$ are symmetry-forbidden. Oscillator strength (length form [a.u. × 100]) in parentheses. [b] Transition energies calculated with FOCI calculations on the CAS(8/11) reference space. All 49 virtual orbitals were included in the calculations. Oscillator strength (length form [a.u. × 100]) in parentheses. [c] Main one-electron excitations from the reference state. [d] Orbitals up to $2b_1$ were kept frozen. Oscillator strength (a.u. × 100) in parentheses. SOMO–LUMO transition is in boldface.

namical electron correlation has a large effect on the calculated transition energies. The FOCI results are intermediate between the CAS-CI and MR-PT ones, and the MR-PT energies are always the lowest. Transition energies calculated with the STS procedure are in nice agreement with the MR-PT results, while higher energies are calculated with TDDFT. The absorption spectrum of SQ^- consists of three bands: that of lowest energy is a $\pi^*\rightarrow$SOMO ($3a_2\rightarrow3b_1$) transition, the central band contains the SOMO$\rightarrow$LUMO ($3b_1\rightarrow4b_1$) and SOMO$\rightarrow$LUMO+1 ($3b_1\rightarrow4a_2$) transitions, and the third band is formed by the $2a_2\rightarrow3b_1$ and $2b_1\rightarrow3b_1$ transitions. The $^2B_1$ states formed by the Slater determinants with $3b_1\rightarrow4b_1$ and $2b_1\rightarrow3b_1$ excitations are mixed by configuration interaction. The mixing becomes more relevant in the zinc complex, where it is close to 50% (see Table 2), and causes a splitting of these transitions larger than that calculated for the free SQ^- radical anion. The SOMO$\rightarrow$LUMO transitions calculated within the STS formalism and by TDDFT for the Zn^{II} complex were 32153 and 36915 cm^{-1}, respectively. The STS result is closer to the MR-PT value than the TDDFT result, as already found for SQ^-. The deviations of both STS and TDDFT from the MR-PT values increase with increasing energy of the transitions. The higher energy states are, on average, more affected by CI mixing than the lower energy ones.

From Table 2 it can be seen that no charge-transfer state that can be assigned to CAT–Zn^{III} species is calculated at energies below 50000 cm^{-1}.

Multiplet structure of $[(NH_3)_2Cu^{II}(SQ)]^+$: According to the energy levels shown in Figure 2, the ground state of $[(NH_3)_2Cu^{II}(SQ)]^+$ arises from the $(1b_2^1\ 3b_1^1)$ configuration and can be either $^3A_2$ or $^1A_2$. The magnetic properties of the complex are tuned by the energy separation between these two states. Application of the BS approach by using Equation (1) yields $^3A_2$ as the ground state and $J=-774$ cm^{-1} [41] (ADF/BP) and -909 cm^{-1} (NWChem/B3LYP). CAS-CI and MR-PT calculations on CAS(13/20) gave $J=-665$ and -384 cm^{-1}, respectively. The J values calculated with DFT/BS are closer to the MR-PT value if the factor of two in Equation (1) is omitted, as was already suggested.[27] In this case one obtains $J=-387$ (ADF/BP) and -454 cm^{-1} (NWChem/B3LYP). A number of dioxolene copper(II) complexes have been studied and showed a large ferromagnetic interaction between Cu^{II} and the SQ^- radical anion.[6b,9,42] In the complex $[Cu\{NH(py)_2\}(DTBSQ)]ClO_4$[43] ($NH(py)_2$ = di-2-pyridylamine; DTBSQ = anion of 3,5-di-*tert*-butylbenzo-*o*-sequinone) the Cu^{II} ion is four-coordinate in a roughly square-planar environment, and the measured J value is -220 cm^{-1}. This is reasonably close to the value calculated with MR-PT.

Calculations of excited triplet states relevant to the interpretation of the UV/Vis spectra were performed by means of CAS-CI calculations on the lowest 50 excited states. The zeroth-order energies of the states with nonzero oscillator strengths at the CAS-CI level were then corrected with MR-PT, and the results of the calculations are reported in Table 4. The calculated low-energy bands are in nice agreement with those reported[44] at 12400 and 25600 cm^{-1} for $[Cu\{NH(py)_2\}(DTBSQ)](ClO_4)$, and also with the transitions observed in the five-coordinate complex[42a] $[Cu(Me_3[12]N_3)(DTBSQ)]ClO_4$ (17500 cm^{-1}, 23300 cm^{-1}, 26900 cm^{-1}, 33200 cm^{-1}; $Me_3[12]N_3$ = 2,4,4-trimethyl-1,5,9-triazacyclododec-1-ene). The transitions at 18170 and 27540 cm^{-1} have pronounced 3d metal character and are assigned as d–d transitions in Table 4. The $^3B_1$ state that originates from the $1a_2\rightarrow3b_1$ excitation from the ground Slater determinant (30147 cm^{-1}) can be assigned as the first triplet excited state corresponding to a CAT/hs-Cu^{III} species (hs = high-spin configuration). Excited states with large charge transfer from the radical ligand to the metal center and vice versa can be obtained from the state configurations $(1b_2^0\ 3b_1^2)$ and $(1b_2^2\ 3b_1^0)$, which originate from $^1A_1$ states that correspond to the ground states of Cu^I–Q and Cu^{III}–CAT species, respectively. Their energies at the MR-PT level are 7163 and 13615 cm^{-1} relative to the $^3A_2$ ground state.

Table 4. Calculated electronic transitions [cm^{-1}] for $[Cu(NH_3)_2(SQ)]^+$.

Transition	CAS[a]	MR-PT	Transition[b]
$^3A_2\rightarrow{}^3B_1$	16280 (1.32)	10645	$3a_2\rightarrow3b_1$
$^3B_1$	*14630* (*0.39*)	*18170*	*$2a_1\rightarrow2b_2$*
$^3B_1$	40078 (0.04)	25792	$2a_2\rightarrow3b_1$
$^3B_1$	42027 (3.91)	**26205**	**$3b_1\rightarrow4a_2$**
$^3A_2$	33130 (3.69)	27236	$2b_1\rightarrow3b_1$
$^3B_1$	*55940* (*5.01*)	*27540*	*$3a_1\rightarrow2b_2$*
$^3A_2$	46891 (7.08)	**28494**	**$3b_1\rightarrow4b_1$**
$^3B_1$	50566 (17.85)	29048	$1b_2\rightarrow3b_1$
$^3B_1$	46228 (0.66)	30147	$1a_2\rightarrow3b_1$
$^3A_2$	57847(16.96)	33100	$1b_2\rightarrow2b_2$
$^3A_2$	43401(0.19)	33436	$3a_1\rightarrow3b_1$
$^3A_2$	49495(2.62)	44105	$1b_1\rightarrow3b_1$

[a] Transition energies from configuration interaction on the CAS(13/20) reference space. Transitions $2A_2\rightarrow2A_1$ are symmetry-forbidden. Oscillator strength (length form [a.u.×100]) in parentheses. [b] Main one-electron excitations. d–d transitions are in italics. SOMO–LUMO transitions are in boldface.

Multiplet structure of $[(NH_3)_4Ni^{II}(SQ)]^+$: Up to 20 states with different spin multiplicity and/or space symmetry can arise from the ground state configuration $(3b_1^1b_2a_1)^3$ of $[(NH_3)_4Ni^{II}(SQ)]^+$; they are listed in Table 5, where their description in terms of localized electrons is also given. In this case the CAS is formed by 13 orbitals and 19 active electrons [CAS(13/19)]. The first two $^2A_2$ states can be designated as the antiferromagnetic state of the couple SQ/hs-

Table 5. Electronic states arising from the ground configuration of $[Ni(NH_3)_4(SQ)]^+$.

System[a]	Configuration	State
SQ/hs-Ni^{II}	$(3b_1^1\ 1b_2^1\ 2a_1^1)$	$^4A_2$
	$(3b_1^\beta\ 1b_2^\alpha\ 2a_1^\alpha)$	$^2A_2$
SQ/ls-Ni^{II}	$(3b_1^\alpha\ 1b_2^\alpha\ 2a_1^\beta)$	$^2A_2$
	$(3b_1^1\ 1b_2^0\ 2a_1^2)$	$^2B_1$
	$(3b_1^1\ 1b_2^2\ 2a_1^0)$	$^2B_1$
CAT/Ni^{III}	$(3b_1^2\ 1b_2^1\ 2a_1^0)$	$^2B_2$
	$(3b_1^2\ 1b_2^0\ 2a_1^1)$	$^2A_1$
Q/Ni^I	$(3b_1^0\ 1b_2^2\ 2a_1^1)$	$^2A_1$
	$(3b_1^0\ 1b_2^1\ 2a_1^2)$	$^2B_2$

[a] The chemical system is described in a localized-electrons picture. hs/ls = high-/low-spin configuration of the metal ion.

Ni^{II} and one state of the SQ/ls-Ni^{II} system, respectively. Since states with the same spin and space symmetry can be strongly mixed by CI, the above "chemical" classification is only loosely correct. Nevertheless, this classification is widely used by chemists to identify the so-called valence tautomers, and we continue to use it in the text. A number of states arising from excitation of the inner electrons and from excitation of the valence electrons to virtual states are also possible. It is evident how the multiplet structure of this system becomes complicated. Therefore, we will not attempt to describe the whole multiplet structure of the $[Ni(NH_3)_4(SQ)]^+$ cation, and we limit the calculations to the description of the states relevant to the interpretation of the electronic spectrum of the $[Ni(NH_3)_4(SQ)]^+$ cation and of the lower lying doublet states listed in Table 6, which can be important for understanding the photochemical properties of the system.[45]

Table 6. The lowest lying doublet states of $[Ni(NH_3)_4(SQ)]^+$ calculated with MR-PT.

State	Energy [cm^{-1}][a]	Description
$^2A_2$	357	SQ/hs-Ni^{II} AF
$^2B_2$	8940	$(1b_1^{\alpha}\ 3b_1^{\beta}\ 1b_2^{\alpha}\ 2a_1^2)$ SQ/ls-Ni^{II}
$^2B_2$	11011	$(3b_1^2\ 1b_2^1\ 2a_1^0)$ CAT/Ni^{III}
$^2A_1$	12868	$(3a_2^{\alpha}\ 3b_1^{\beta}\ 1b_2^{\alpha}\ 2a_1^2)$ Q/Ni^{I}

[a] Energy difference from the $^4A_2$ ground state.

The ground state of the system, $^4A_2$, agrees with the ferromagnetic interaction between SQ^- and Ni^{II} experimentally observed in the real systems.[7] The nearest doublet state was calculated to be the $^2A_2$ state arising from the SQ/hs-Ni^{II} system. Its MR-PT energy of 357 cm^{-1} relative to the ground state can be compared with that obtained by using the spin Hamiltonian $\Delta E = E(S=3/2) - -E(S=1/2) = 3J/2$, which yields $J = -238\ cm^{-1}$. This value agrees with the ferromagnetism observed in the $[Ni(CTH)(DBSQ)]^+$ and $[Ni(CTH)(PhenSQ)]^+$ cations, and compares well with the values calculated for these complexes at the DFT/B3LYP level, that is, -356 and $-285\ cm^{-1}$.[11f] The J values calculated from Equation (1) are -637 (ADF/BP) and $-468\ cm^{-1}$ (NWChem/B3LYP). Without application of the spin projection, the calculated J values are -424 (ADF/BP) and $-312\ cm^{-1}$ (NWChem/B3LYP). The latter value agrees well with that calculated by the MR-PT approach. The comparison of the J values calculated for our model system with those calculated for two chemical systems, that is, $-312\ cm^{-1}$ versus -356 and $-285\ cm^{-1}$, shows that the modelling introduced in the present paper does not significantly alter the value of the exchange coupling constant.

The next excited doublet state was found at 8940 cm^{-1} from the ground state, and it will not be thermally populated at room temperature. Using the Slater determinant with the largest coefficient in the CAS-CI zeroth-order state, that is 0.653, this state is labelled SQ/ls-Ni^{II}. Its one-electron picture differs from that expected from the ground state configuration of Table 5 due to relevant effects of electron–electron interactions. However an excited $^2B_1$ state was calculated at 16515 cm^{-1}, as a linear combination of the Slater determinants arising from the configurations $(3b_1^1\ 1b_2^0\ 2a_1^2)$ and $(3b_1^1\ 1b_2^2\ 2a_1^0)$ with coefficients of 0.673 and 0.641, respectively. Similar considerations can be drawn for the other excited states.

Many excited states with $S = 3/2$ arise from a CAS(13/19). To interpret the electronic absorption spectra of the SQ/Ni^{II} system we adopted the same protocol as for the Cu^{II} system, that is, we calculate a large number of quartet states at the CAS-CI level, and we correct with MR-PT only those states which have transitions moments significantly different from zero. The results of these calculations for states lying below about 55000 cm^{-1} are summarized in Table 7. The assignment of the transitions to one-electron excitations is somewhat arbitrary, since in many cases the excited states are strongly mixed by configuration interaction. Indeed, for most of the highest energy transitions, an assignment was not possible. The states classified as MLCT correspond, in chemical language, to excited CAT/hs-Ni^{III} states.

Table 7. Calculated electronic transitions [cm^{-1}] for $[Ni(NH_3)_4(SQ)]^+$.

Transition	MR-PT[a]	Transition[b]	Exptl[c]	
$^4A_2 \rightarrow {}^4B_2$	*9251 (0.01)*	*$1b_1 \rightarrow 2a_1$*		
$^4B_1$	13004 (2.80)	3a→3b1	11400	12950
$^4B_1$	*15181 (0.01)*	*$3a_1 \rightarrow 1b_2$*		
$^4A_2$	18967 (4.8)	$1b_1 \rightarrow 3b_1$ MLCT		
$^4A_2$	*20933 (0.01)*	*$3a_1 \rightarrow 2a_1$*	19200	21200
$^4B_1$	**21816 (1.60)**	**$3b_1 \rightarrow 4a_2$**		
$^4B_2$	*22913 (0.01)*	*$1b_1 \rightarrow 2a_1$*		
$^4A_2$	24925 (1.80)	$2b_1 \rightarrow 3b_1$		
$^4B_1$	26551 (22.7)	$2a_2 \rightarrow 3b_1$	24760	
$^4B_1$	28092 (0.17)	M		
$^4A_2$	**28892 (13.89)**	**$3b_1 \rightarrow 4b_1$**	29700	32380
$^4B_1$	32010 (0.25)	$1a_2 \rightarrow 3b_1$ MLCT		
$^4A_2$	33447 (0.04)	M		
$^4A_2$	34507 (0.02)	*$3a_1 \rightarrow 2a_1$*		
$^4B_2$	34708 (0.02)	$3a_2 \rightarrow 1b_2$ LMCT		
$^4A_2$	37295 (0.31)	M		
$^4B_1$	38973 (0.19)	M		
$^4A_2$	38976 (0.02)	M		
$^4B_1$	39465 (0.01)	M		
$^4A_2$	40775 (0.06)	$3a_2 \rightarrow 4a_2$		
$^4B_1$	47457 (0.73)	M		
$^4B_2$	55495 (2.86)	M		

[a] Transitions $2A_2 \rightarrow 2A_1$ are symmetry-forbidden. Oscillator strength (length form [a.u. × 100]) in parentheses taken from CAS-CI(13/19) calculations. [b] Main one-electron excitations from the reference configuration. d–d transitions are in italics. SOMO–LUMO transitions are in boldface. MLCT = metal-to-ligand charge transfer. LMCT = ligand-to-metal charge transfer. M = multiple transitions. [c] Data taken from the spectra of $[Ni(SS\text{-}CTH)(TCSQ)]ClO_4$ (left) and $[Ni(SS\text{-}CTH)(DTBSQ)]PF_6$ (right) from ref. [40] Only the most intense transitions are reported.

Conclusion

The combined use of DFT and MR-PT theory allowed us to calculate the spectromagnetic properties of a series of model complexes of Zn, Cu and Ni with a paramagnetic semiquinonato ligand, with reasonably good agreement with experimental findings and a reasonably low CPU cost/accuracy ratio. The KS orbitals obtained from restricted open-shell DFT/B3LYP calculations were used as basis for the

CAS, and the success of the calculations can be related to the ability of DFT to account for a large part of the dynamic correlation effects, which yields wavefunctions that represent the ground state of the system better than their Hartree–Fock counterparts. Correlation interactions on the reference CAS and MR-PT theory are apparently good enough to account for almost all of the static correlation.

Standard DFT techniques (BS, STS) gave results comparable to the MR-PT approach for the calculation of the *J* values, but larger differences in the electronic spectra were obtained. The STS procedure gave better energies than TDDFT in the cases we examined. Another result of some importance in magnetochemistry that resulted from our calculations is that the *J* values calculated without using the spin projection of the BS state are closer to the values calculated with the MR-PT theory when the B3LYP functional is applied. This result supports the procedure sometimes used in the literature, that is, to omit this spin projection.

Further calculations are still required to more completely validate the present approach in the study of the physicochemical properties of metal dioxolene complexes. In particular the choice of the basis states for the CAS has to be investigated by performing calculation with unrestricted wavefunctions and, consequently, unrestricted natural orbitals (UNO).

With the present model we have calculated the complex electronic structure of simple chemical models. Application of this model to the calculation of complex electronic structures of molecular systems of chemical complexity is a future challenge.

Some important predictions can be made from our present results. In the copper and nickel systems we calculated excited states with spin multiplicities different from that of the ground state at relatively low energies, namely, Q/Cu^{I} and CAT/Ni^{III} at 7163 and 11011 cm^{-1}, respectively. Since these energies are Frank–Condon energies they represent an upper limit to the energies of the states when geometrical relaxation is allowed for. Note, for example, that Cu^{I} prefers pseudotetrahedral coordination, and structural variations are important in stabilizing the various oxidation states.[8a] These states, even if not available to valence tautomerism because they are higher in energy than the thermal quantum, could be populated by photoexcitation with laser pumps and could give rise to long-lived excited species, and to peculiar photochemical properties.

Calculations on more complex systems, namely complexes of Co, Fe and Mn, are planned, as well as the use of DFT to optimize the geometrical structures of the excited states in order to go beyond the Frank–Condon approximation.

Acknowledgment

The authors are indebted to Prof. Andrea Dei, Università di Firenze, for his continuous stimulation during the work and for the many helpful, even if sometimes heated, discussions. Financial support from Deutsche Forschungsgemeinschaft (DFG), Molekularer Magnetismus (SPP1137), MOLNANOMAG HPRN-CT-1999-00012, SENTINEL HPRU-CT-2000-40022, High Field ICN HPRI-CT-1999-40013, HPMF-CT-2002-02159, and MIUR are gratefully acknowledged.

[1] *Reviews of Modern Quantum Chemistry, Vols. 1, 2* (Ed.: K. D. Sen) World Scientific, Singapore, **2002**.
[2] F. Jensen, *Introduction to Computational Chemistry*, Wiley, Chichester, **1999**.
[3] J. Harris, *Phys. Rev.* **1984**, *29*, 1648.
[4] *Recent Advances in Density Functional Methods, Part III* (Eds: V. Barone, A. Bencini, P. Fantucci), World Scientific, Singapore, **2002**.
[5] *Magnetism: Molecules to Materials* (Eds: J. S. Miller, M. Drillon), Wiley-VCH, Weinheim, **2001**.
[6] a) D. Gatteschi, *Adv. Mater.* **1994**, *6*, 635; b) C. G. Pierpont, A. S. Attia, *Collect. Czech. Chem. Commun.* **2001**, 66; c) A. Bencini, A. Caneschi, A. Dei, D. Gatteschi, C. Sangregorio, D. Shultz, L. Sorace, M. G. F. Vaz, *C. R. Chim.* **2003**, *6*, 663.
[7] A. Dei, D. Gatteschi, *Inorg. Chim. Acta* **1992**, *198–200*, 813.
[8] a) C. G. Pierpont, *Coord. Chem. Rev.* **2001**, *219–221*, 99; b) C. G. Pierpont, C. W. Lange, *Progr. Coord. Chem.* **1993**, *41*, 381; c) P. Guetlich, A. Dei, *Angew. Chem.* **1997**, *109*, 2852; *Angew. Chem. Int. Ed. Engl.* **1997**, *36*, 2734; d) D. A. Shultz in *Magnetism: Molecules to Materials* (Eds: J. S. Miller, M. Drillon), Wiley-VCH, Weinheim, **2001**; e) D. M. Adams, A. L. Rheingold, D. N. Hendrickson, *J. Am. Chem. Soc.* **1993**, *115*, 8221.
[9] C. G. Pierpont, R. M. Buchanan, *Coord. Chem. Rev.* **1981**, *38*, 87.
[10] W. Kohn, A. D. Becke, R. G. Parr, *J. Phys. Chem.* **1996**, *100*, 12974.
[11] a) D. M. Adams, L. Noodleman, D. N. Hendrickson, *Inorg. Chem.* **1997**, *36*, 3966; b) J. H. Rodriguez, D. E. Wheeler, J. K. McCusker, *J. Am. Chem. Soc.* **1998**, *120*, 12051; c) Y. Pontillon, A. Bencini, A. Caneschi, A. Dei, D. Gatteschi, B. Gillon, C. Sangregorio, J. Stride, F. Totti, *Angew. Chem. Int. Ed.* **2000**, *39*, 1786; d) A. Bencini, C. A. Daul, A. Dei, F. Mariotti, H. Lee, D. A. Shultz, L. Sorace, *Inorg. Chem.* **2001**, *40*, 1582; e) V. Bachler, G. Olbrich, F. Neese, K. Wieghardt, *Inorg. Chem.* **2002**, *41*, 4179; f) A. Bencini, C. Carbonera, A. Dei, M. G. F. Vaz, *J. Chem. Soc. Dalton Trans.* **2003**, 1701.
[12] A. Bencini, C. Carbonera, A. Dei, *Proceedings of the VIII International Conference on Molecule-based Magnets* (ICMM), Valencia, Spain, **2002**, F-16.
[13] M. X. LaBute, R. V. Kulkarni, R. G. Endres, D. L. Cox, *J. Phys. Chem.* **2002**, *116*, 3681.
[14] a) R. Pollet, A. Savin, T. Leininger, H. Stoll, *J. Chem. Phys.* **2002**, *116*, 1250; b) R. Takeda, S. Yamanaka, K. Yamaguchi, *Chem. Phys. Lett.* **2002**, *366*, 321; c) S. Grimme, M. Waletzke, *J. Chem. Phys.* **1999**, *111*, 5645.
[15] P. Bour, *Chem. Phys. Lett.* **2001**, *345*, 331.
[16] A. Caneschi, A. Dei, F. Fabrizi de Biani, P. Guetlich, V. Ksenofontov, G. Levchenko, A. Hoefer, F. Renz, *Chem. Eur. J.* **2001**, *7*, 3926.
[17] a) E. J. Baerends, D. E. Ellis, P. Ros, *Chem. Phys.* **1973**, *2*, 41; b) G. te Velde, E. J. Baerends, *J. Comput. Phys.* **1992**, *99*, 84; c) C. Fonseca Guerra, J. G. Snijders, G. te Velde, E. J. Baerends, *Theor. Chem. Acc.* **1998**, *99*, 39.
[18] GAMESS, Version 20, June **2002**; M. W. Schmidt, K. K. Baldridge, J. A. Boatz, S. T. Elbert, M. S. Gordon, J. H. Jensen, S. Koseki, N. Matsunaga, K. A. Nguyen, S. Su, T. L. Windus, M. Dupuis, J. A. Montgomery, *J. Comput. Chem.* **1993**, *14*, 1347.
[19] High Performance Computational Chemistry Group, NWChem, A computational chemistry package for parallel computers, Version 4.5, Pacific Northwest National Laboratory, Richland, Washington, **2003**.
[20] a) A. Schafer, C. Huber, R. Ahlrichs, *J. Chem. Phys.* **1994**, *100*, 5829; b) A. Schafer, H. Horn, R. Ahlrichs, *J. Chem. Phys.* **1992**, *97*, 2571.
[21] Extensible computational chemistry environment basis set database, Version 4/17/03, as developed and distributed by the Molecular Science Computing Facility, Environmental and Molecular Sciences Laboratory, which is part of the Pacific Northwest Laboratory, P. O. Box 999, Richland, Washington 99352, USA, and funded by the U.S. Department of Energy. The Pacific Northwest Laboratory is a multiprogram laboratory operated by Battelle Memorial Institute for the U.S. Department of Energy under contract DE-AC06-76RLO 1830.
[22] S. H. Vosko, L. Wilk, M. Nusair, *Can. J. Phys.* **1980**, *58*, 1200.
[23] A. D. Becke, *Phys. Rev.* **1988**, *38*, 3098.
[24] J. P. Perdew, *Phys. Rev.* **1986**, *33*, 8822.
[25] a) I. Ciofini, C. A. Daul, A. Bencini in *Recent Advances in Density Functional Methods*, (Eds.: V. Barone, A. Bencini, P. Fantucci), Part

III, World Scientific, Singapore, **2002**, 106; b) L. Noodleman, C. Y. Peng, D. A. Case, J. M. Mouesca, *Coord. Chem. Rev.* **1995**, *144*, 199; c) L. Noodleman, D. A. Case, S. F. Sontum, *J. Chem. Phys.* **1989**, *86*, 743; d) A. Bencini, *J. Chem. Phys.* **1989**, *86*, 763; e) L. Noodleman, *J. Chem. Phys.* **1981**, *74*, 5737; f) L. Noodleman, J. G. Norman, Jr., *J. Chem. Phys.* **1979**, *70*, 4903.

[26] Several forms of the spin Hamiltonian are in use among magnetochemists that differ in the form of the constant factor, which can take the form: $-J$, $-2J$, or $2J$. In this paper all the experimental data have been transformed to our convention.

[27] a) T. Soda, Y. Kitagawa, T. Onishi, Y. Takano, Y. Shigeta, H. Nagao, Y Yoshioka, K. Yamaguchi, *Chem. Phys. Lett.* **2000**, *319*, 223; b) E. Ruiz, J. Cano, S. Alvarez, P. Alemany, *J. Comput. Chem.* **1999**, *20*, 1391.

[28] a) D. R. Gamelin, E. L. Bominaar, M. L. Kirk, K. Wieghardt, E. I. Solomon, *J. Am. Chem. Soc.* **1986**, *108*, 8085; b) V. Barone, A. Bencini, I. Ciofini, C. A. Daul, F. Totti, *J. Am. Chem. Soc.* **1998**, *120*, 8357.

[29] C. Adamo, V. Barone, A. Bencini, F. Totti, I. Ciofini, *Inorg. Chem.* **1999**, *38*, 1996.

[30] J. C. Slater, *The Self-Consistent Field for Molecules and Solids, Quantum Theory of Molecules and Solids, Vol. 4*, McGraw-Hill, New York, **1974**.

[31] M. W. Schmidt, M. S. Gordon, *Ann. Rev. Phys. Chem.* **1998**, *49*, 233.

[32] a) A. D. Becke, *J. Chem. Phys.* **1993**, *98*, 5648; b) P. J. Stephens, F. J. Devlin, C. F. Chablowski, M. J. Frisch, *J. Phys. Chem.* **1994**, *98*, 11623; c) R. H. Hertwig, W. Koch, *Chem. Phys. Lett.* **1997**, *268*, 345.

[33] a) K. Hirao, *Chem. Phys. Lett.* **1992**, *190*, 374; b) K. Hirao, *Chem. Phys. Lett.* **1992**, *196*, 397; c) K. Hirao, *Int. J. Quant. Chem.* **1992**, *S26*, 517; d) K. Hirao, *Chem. Phys. Lett.* **1993**, *201*, 59.

[34] a) H. Nakano, K. Nakayama, K. Hirao, M. Dupuis, *J. Chem. Phys.* **1997**, *106*, 4912; b) T. Hashimoto, H. Nakano, K. Hirao, *J. Mol. Struct.* **1998**, *451*, 25.

[35] a) K. R. Glaesemann, M. S. Gordon, H. Nakano, *J. Chem. Phys.* **1999**, *1*, 967; b) Y.-K. Choe, H. A. Witek, J. P. Finley, K. Hirao, *J. Chem. Phys.* **2001**, *114*, 3913; c) H. A. Witek, D. G. Fedorov, K. Hirao, A. Viel, P.-O. Widmark, *J. Chem. Phys.* **2002**, *116*, 8396.

[36] a) C. Jamorski, M. E. Casida, D. R. Salahub, *J. Chem. Phys.* **1996**, *104*, 5134; b) R. Bauernschmitt, R. Ahlrichs, *Chem. Phys. Lett.* **1996**, *256*, 454; c) R. Bauernschmitt, M. Häser, O. Treutler, R. Ahlrichs, *Chem. Phys. Lett.* **1997**, *264*, 573.

[37] S. Hirata, M. Head-Gordon, *Chem. Phys. Lett.* **1999**, *314*, 291.

[38] J. S. Thompson, J. C. Calabrese, *Inorg. Chem.* **1985**, *24*, 3167.

[39] D. E. Wheeler, J. H. Rodriguez, J. K. McCusker, *J. Phys. Chem.* **1999**, *103*, 4101.

[40] C. Benelli, A. Dei, D. Gatteschi, L. Pardi, *Inorg. Chem.* **1989**, *28*, 1476.

[41] In the case of two interacting $S=1/2$ spins, J is equal to the singlet–triplet splitting.

[42] a) C. Benelli, A. Dei, D. Gatteschi, L. Pardi, *Inorg. Chem.* **1990**, *29*, 3409; b) C. G. Pierpont, C. V. Lange, *Prog. Chem.* **1994**, *41*, 331; c) G. Speier, J. Csihony, A. M. Whalen, C. G. Pierpont, *Inorg. Chem.* **1996**, *35*, 3519.

[43] O. Kahn, R. Prins, J. Reedijk, J. S. Thompson, *Inorg. Chem.* **1987**, *26*, 3557.

[44] J. S. Thompson, J. C. Calabrese, *Inorg. Chem.* **1985**, *24*, 3167.

[45] F. Neuwahl, R. Righini, A. Dei, *Chem. Phys. Lett.* **2002**, *352*, 408.

Received: August 1, 2003
Revised: November 7, 2003 [F5420]